Available online at www.sciencedirect.com
SCIENCE DIRECT®
Journal of Magnetic Resonance 160 (2003) 33–39
JMR Journal of Magnetic Resonance
www.elsevier.com/locate/jmr

Structural fitting of PISEMA spectra of aligned proteins

Alexander A. Nevzorov and Stanley J. Opella*

Department of Chemistry and Biochemistry, University of California at San Diego, 9500 Gilman Drive, La Jolla, CA 92093-0307, USA

Received 17 April 2002; revised 8 August 2002

Abstract

An algorithm for fitting protein structures to PISEMA spectra is described, and its application to helical proteins in aligned samples is demonstrated using both simulated and experimental results. The formulation of the algorithm in terms of rotation operators yields compact recursion relations that provide a fast and effective way of obtaining peptide plane orientations from chemical and torsion angle constraints. The algorithm in combination with experimental solid-state NMR data results in a method for determining the backbone structures of proteins, since it yields the orientation of a helix as a whole, including its tilt and twist angles, and describes kinks and curves with atomic resolution. Although the algorithm can be applied in an "assignment-free" manner to spectra of uniformly labeled proteins, the precision of the structural fitting is improved by the addition of assignment information, for example the identification of resonances by residue type from spectra of selectively labeled proteins.

Keywords: Solid-state NMR; PISEMA; Torsion angles; Angular constraints; Protein structure; PISA wheel

1. Introduction

Solid-state NMR spectra of aligned samples display a direct mapping of the structures of a protein into the patterns of resonance frequencies. This is exemplified by PISA (polarity index slant angle) [1,2] wheels of α-helices in two-dimensional PISEMA (polarization inversion spin exchange at the magic angle) [3] spectra, but can be generalized to all types of secondary structure and multi-dimensional NMR spectra [4,5]. The main goal of NMR studies of aligned proteins is to determine their three-dimensional structures directly from experimental solid-state NMR data; however, this process is complicated by the fact that, due to an even rank of the dipolar and chemical shift interaction tensors, multiple orientations are consistent with each frequency in a solid-state NMR spectrum [6].

Structure determination by NMR traditionally follows the path of resolving resonances from individual sites, measuring spectral parameters indicative of structure, assigning the resonances, and only then calculating the structure. Here, we describe the use of structural fitting as an alternative approach to determining protein structures from solid-state NMR data of aligned samples. It has the novel feature of treating the resonance assignments as an adjustable parameter. Further, selective isotopic labeling by residue type can restrict the assignments to a limited number of resonances and improve the quality of fit. All of the residues are linked to each other in a specific chemical manner (peptide bonds) and in defined order (sequence), which provide intrinsic orientational and structural constraints that supplement those from the experimental NMR spectral frequencies. A considerable amount of information about the overall orientation and conformation of a peptide domain can be derived from the appearance of the solid-state NMR spectra; taken together, these constraints can give a close set of structures which, in the most complete implementation of the algorithm, fit the solid-state NMR spectrum in an "assignment-free" manner.

We focus on two-dimensional $^{1}H/^{15}N$ PISEMA spectra [3] because of their applicability to proteins expressed in bacteria. In this initial investigation, we focus on spectra from helical domains of uniformly ^{15}N-labeled proteins that are immobile on the timescales of the spin interactions and completely aligned in the magnetic field of the NMR spectrometer.

* Corresponding author. Fax: 1-858-822-4821.
E-mail address: sopella@ucsd.edu (S.J. Opella).

1090-7807/02/$ - see front matter © 2002 Elsevier Science (USA). All rights reserved.
PII: S1090-7807(02)00138-6

2. Results and discussion

2.1. Geometry of peptide chains and solid-state NMR frequencies

In order to carry out a structural fitting to the NMR data, it is necessary to relate the geometry of a peptide to its NMR spectrum. This starts with the definition of a chain propagator that "walks" across the spectrum from the resonance of one residue (i) to that of the next residue in the sequence $(i+1)$. Mathematically, the chain propagator calculates the orientation of the applied magnetic field $\mathbf{B_0}$ relative to the $(i+1)$th peptide plane $(\alpha_{i+1}, \beta_{i+1})$ on the basis of its orientation relative to the preceding peptide plane (α_i, β_i) and the torsional angles Φ_i and Ψ_i between these two planes. In contrast to the approach of Denny et al. [7], which employs a Cartesian basis, we utilize an irreducible representation of rotations. The chain propagator can then be expressed in terms of the Wigner rotation matrices that operate on the basis of spherical harmonics

$$\mathbf{Y}^{\mathrm{T}}(\beta_{i+1}, \alpha_{i+1}) = \mathbf{Y}^{\mathrm{T}}(\beta_i, \alpha_i)\mathbf{P}(\Phi_i, \Psi_i). \tag{1}$$

Here the indexing of Φ and Ψ takes into account the variations in their values along the chain. The vector $\mathbf{Y}$ is given in terms of (unnormalized) spherical harmonics of rank 1 by

$$\mathbf{Y}(\beta,\alpha) \equiv \begin{pmatrix} Y_1^{(1)}(\beta,\alpha) \\ Y_0^{(1)}(\beta,\alpha) \\ Y_{-1}^{(1)}(\beta,\alpha) \end{pmatrix}, \quad Y_0^{(1)}(\beta,\alpha) = \cos\beta, \qquad Y_{\pm1}^{(1)}(\beta,\alpha) = \mp\frac{\sin\beta}{\sqrt{2}}\mathrm{e}^{\pm\mathrm{i}\alpha}. \tag{2}$$

The propagator matrix $\mathbf{P}(\Phi, \Psi)$ is given by a product of two Wigner rotation matrices of rank 1 tabulated by Arfken [8]

$$\mathbf{P}(\Phi,\Psi) = \mathbf{D}^{(1)}(151.8^\circ, \Phi, 109.47^\circ) \times \mathbf{D}^{(1)}(0, -\Psi - 180^\circ, 34.9^\circ). \tag{3}$$

The propagator brings the molecular frame (MF) associated with peptide plane (i) into coincidence with the molecular frame of the following residue $(i+1)$ as illustrated in Fig. 1. The first Euler angle in the first Wigner matrix of Eq. (3) is the angle between the y-axis of the MF and the N–C_α bond of the ith plane; the third Euler angle in the first Wigner matrix is the tetrahedral angle; finally, the third Euler angle in the second Wigner matrix is the angle between the C_α–C bond and the y-axis of the MF of the $(i+1)$th plane. The numerical values for the corresponding Euler angles reflect the geometry of a standard peptide plane [9] and are assumed to be constant, regardless of the residue type or position in the sequence. This enables the entire protein backbone to be reconstructed from the values of the torsional angles Φ_i and Ψ_i. For example, setting $\Phi = -65^\circ$ and $\Psi = -40^\circ$ in successive applications of Eq. (1) results in an ideal α-helix.

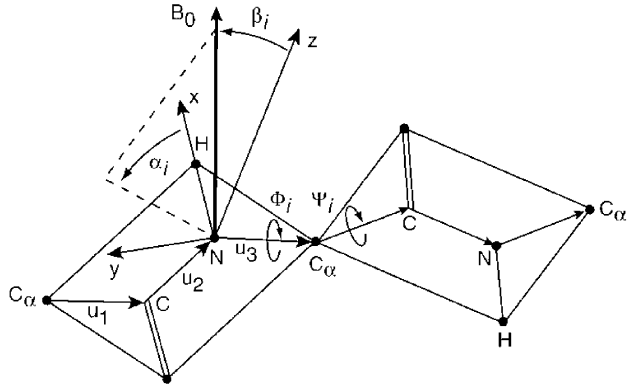

Fig. 1. The molecular frame xyz and the directional vectors $\mathbf{u}_k$ $(k = 1, 2, 3)$ for a peptide plane. The orientation of the magnetic field $\mathbf{B_0}$ relative to the molecular frame of the ith peptide plane is described by the angles α_i and $(\beta_i$. The torsional angles Φ_i and Ψ_i are used to describe the relative orientation of the molecular frames of the ith and $(i+1)$th planes, cf. the text. The numerical values for the relevant bond lengths and angles are taken from [9]. The N–H bond length is assumed to be 1.07 Å.

Each resonance in a two-dimensional PISEMA spectrum of a ^{15}N-labeled protein in an aligned sample is characterized by two orientationally dependent frequencies, the ^{15}N chemical shift and the ^{1}H–^{15}N heteronuclear dipolar coupling. These frequencies are given in terms of the angles α_i and β_i that define the orientation of the applied magnetic field, $\mathbf{B_0}$, relative to the MF of the ith peptide plane (cf. Fig. 1) by

$$\begin{aligned} \nu_i(^{15}\mathrm{N}) &= \sigma_{11}\sin^2\beta_i\sin^2(\alpha_i-\gamma) + \sigma_{22}\cos^2\beta_i \\ &\quad + \sigma_{33}\sin^2\beta_i\cos^2(\alpha_i-\gamma), \\ \nu_i(^{15}\mathrm{H}\text{–}^{15}\mathrm{N}) &= \pm\frac{\gamma_\mathrm{N}\gamma_\mathrm{H}\hbar}{r_{\mathrm{N-H}}^3}\,\frac{3\sin^2\beta_i\cos^2\alpha_i - 1}{2}, \end{aligned} \tag{4}$$

where $\gamma = 17^\circ$ is the angle between the x-axis of the MF and the z-axis of the principal axis system (PAS) of the ^{15}N chemical shift tensor [10]. The N–H bond length is taken as $r_{\mathrm{N-H}} = 1.07$ Å. For all residues except glycine and proline, the magnitudes of the principal values for the ^{15}N chemical shift tensor are: $\sigma_{11} = 64$, $\sigma_{22} = 77$, and $\sigma_{33} = 217$ ppm [10]. For glycine $\sigma_{11} = 41$, $\sigma_{22} = 64$, and $\sigma_{33} = 210$ ppm [11]. Proline residues are dealt with separately because of the absence of an amide hydrogen and their different chemical shift parameters.

Each peptide plane is described by three directional vectors $\mathbf{u}_1$, $\mathbf{u}_2$, and $\mathbf{u}_3$, the coordinates of which can be obtained from the peptide plane geometry, cf. Fig. 1. In the irreducible spherical basis, they can be rewritten as

$$\mathbf{u}_k \equiv \begin{pmatrix} -\frac{x_k+\mathrm{i}y_k}{\sqrt{2}} \\ z_k \\ \frac{x_k-\mathrm{i}y_k}{\sqrt{2}} \end{pmatrix}. \tag{5}$$

Here (x_k, y_k, z_k) are the vector coordinates measured relative to the *molecular frame* for the directional vectors ending at the carboxyl carbon, nitrogen, and the α-carbon-labeled by $k = 1$, 2, and 3, respectively.

Relative to the *laboratory frame*, the orientation of the peptide planes is calculated as follows. For the first residue ($i = 1$):

$$\mathbf{v}_k^{(1)\mathrm{T}} = \mathbf{u}_k^{\mathrm{T}}\mathbf{D}^{(1)}(0, \beta_1, \pi - \alpha_1)^{-1}. \quad (6)$$

For subsequent residues, the following recursion relation is applied:

$$\mathbf{v}_k^{(i+1)\mathrm{T}} = \mathbf{v}_k^{(i)\mathrm{T}}\mathbf{P}(\Phi_i, \Psi_i)^{-1}. \quad (7)$$

Taking the inverse of the propagator means that the transformation is now active. It is not the coordinate system, but rather the vectors that are rotated. The backbone structure is finally assembled by adding all the vectors $\mathbf{v}_{\mathrm{k}}^{(i)}$ together in the order specified by the peptide linkages.

The recursive nature of Eqs. (1) and (7) provides a fast, effective way of walking back and forth along the backbone and across the spectrum by taking into account the allowed chemical linkages between the residues.

2.2. The fitting algorithm

To reduce the number of irrelevant backbone conformations resulting from the even parity of the dipolar and chemical shift interactions, torsional angle constraints are utilized. The uniqueness of the structural fit to a spectrum is largely determined by the experimental error and the allowed range for the torsional angles. A PISA wheel inherently contains the information about the torsional angle variations within a helical structure. The more variation allowed in the torsional angles Φ and Ψ, the larger the number of structures that can be fit to a PISEMA spectrum. In contrast, if the torsional angles are allowed to vary too little, then no solution may be found. To obtain a converged set of solutions, the range for the torsional angles must be minimized while still finding a representative number of structures. The goal is to fit the spectrum to the most ideal helical structures possible; smaller deviations from the ideal values for the torsional angles ($\Phi = -65°, \Psi = -45°$) result in more regular hydrogen bonds and in more stable helices.

The steps for the implementing of such a fitting algorithm can be summarized as follows:

0. Arbitrarily label all resonances in the spectrum, e.g., $1, 2, 3, 4, \ldots, N$.
1. Randomly choose a resonance to serve as the starting point and determine the orientation of the magnetic field relative to the MF, i.e. it (α_1, β_1) from Eq. (4).
2. Choose the nearest resonance ($i \geqslant 2$) in the spectrum that satisfies the torsional angle restraints and the selected maximum allowed deviation from the experimental data using Eqs. (1) and (4).
3. Go to the resonance for the next residue $(i + 1)$ as prescribed by step 2.
4. If no resonance can be found that meets the criteria for the $i + 1$ residue, go back to the previous assigned resonance $(i - 1)$ and re-assign the ith resonance as prescribed by step 2.
5. When the resonance assignments are complete for the entire peptide sequence, calculate the structure.
6. Reshuffle the order of the peaks and go back to step 1.
7. Repeat until a converged set of structures is found.

It is important to note that, instead of calculating all (8 in general) possible peptide plane orientations corresponding to each frequency point [12], the orientations are propagated by Eq. (1), which gives no ambiguity with regard to the additional ±180° phase for the angles α_{i+1} and β_{i+1} and their signs. This ambiguity is eliminated by choosing the angles Φ_i and Ψ_i appropriately, so that they satisfy both the angular constraints and the equations for the corresponding frequencies, Eq. (4). These ambiguities remain for step 1; thus, all possible initiations of a helix must be tried out.

If a poor initiation of an α-helix takes place at step 1, then at a later stage of the assignment process there will be no possible α-helical solutions. The algorithm then walks all the way back and re-assigns the resonance corresponding to the first residue. For each ith step of assignment, the magnetic field orientations given by Eq. (2) for the remaining (unassigned) $N - i + 1$ residues and the corresponding torsional angles are stored in memory to speed up the calculations. When the assignment process is complete, the information about the fold of an N-residue peptide and its overall orientation is contained in $N - 1$ pairs of the torsional angles Φ_i and Ψ_i and the angles β_1 and $\pi - \alpha_1$, which define the orientation of the first residue plane. The backbone can then be reconstructed by using Eqs. (6) and (7).

The implementation of the algorithm, including the pictorial representation of three-dimensional peptide backbones, was performed using MATLAB (Mathworks) on a Linux PC operating at 1.7 GHz. The calculation time for each of the structures varies from several minutes to several hours depending on the length of the primary sequence.

2.3. Examples

A PISA wheel for an ideal $\Phi = -65°, \Psi = -40°$) 18-residue α-helix consisting entirely of alanines is shown in Fig. 2a; the corresponding helix structure is shown on the right with a slant angle of approximately 30° between its axis and the direction of the applied magnetic field. In real proteins, the torsional angles vary slightly from the ideal α-helical values. This is illustrated in Fig. 2b with a spectrum calculated with random variations in the values of Φ and Ψ within ±5°, and the corresponding

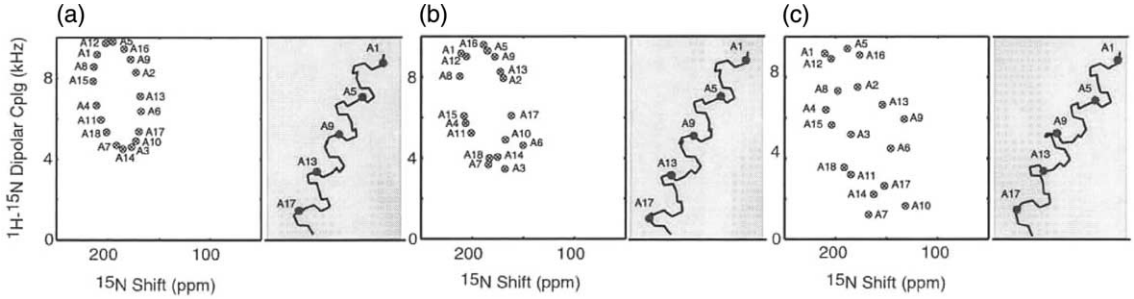

Fig. 2. Effect of the variations in the torsional angles Φ and Ψ on α-helices and their PISEMA spectra. (a) The spectral PISA wheel and structure for an ideal 18-residue α-helix with $\Phi = -65°$ and $\Psi = -40°$. Some spectral peaks are related by arrows to the corresponding ^{15}N atomic positions in the α-helix. (b) The spectrum and structure for a distorted α-helix with random variations in $\Phi = -65° \pm 5°$ and $\Psi = -40° \pm 5°$. (c) The spectrum and structure with variations in $\Phi = -65° \pm 10°$ and $\Psi = -40° \pm 10°$.

structure on the right. Larger variations in Φ and Ψ angles result in more dramatic deviations from an ideal PISA wheel; however, the appearance of the corresponding helical structure and its overall orientation vary only slightly compared to the ideal case. This is illustrated in Fig. 2c with random variations in the values of Φ and Ψ within $\pm 10°$.

Fig. 3a represents the PISA wheel for an ideal helix tilted at 30°, as shown on the left. The structure in the right part of Fig. 3a was back-calculated from the spectrum using the "assignment-free" algorithm described above. The "experimental error" was only 0.01 Hz for both frequencies and the angles Φ and Ψ were allowed to vary within $\pm 5°$. Ten random shuffles of the resonances yielded the same structures shown in Fig. 3a, corresponding exactly to the original α-helix and the correct assignments (i.e., residue 1 is assigned to peak 1, residue 2 to peak 2, etc.). Thus, if the torsional angles are known to a high precision and the data are very accurate, the structural fit may be unique.

By contrast, increasing the fitting range for Φ and Ψ angles to $\pm 10°$ yields structural fits with altered resonance assignments. One such assignment of the spectrum and the corresponding structure are shown in Fig. 3b; a superposition of the structural fits obtained from 10 random shuffles of the resonances is shown in Fig. 3c. The structural fit loses precision as larger limits are put on the Φ and Ψ angles. Notably, even though the resonance assignments are different for each of the fits, the resulting protein structures are very similar with an RMSD of less than 2 Å. This is a striking finding, since it demonstrates that the structural information in the solid-state NMR spectra is contained in the patterns of resonances as well as the individual frequencies.

Structural fitting works best when the helix axis (hence the orientations of N–H bonds) is roughly parallel to the magnetic field because errors in the frequency dimensions yield relatively small errors in the final structures. By contrast, when the helices are close to perpendicular to the magnetic field, small errors in the frequency dimensions give rise to larger structural differences. This is a consequence of the well-known singularities in solid-state NMR, when multiple perpendicular orientations of the z-axis of a PAS yield similar NMR frequencies. This may be overcome with the addition of assignment information, for example assignments of resonances to types of residues or a few sequential assignments.

2.4. Applications to experimental data

Fig. 4 shows the application of the structural fitting algorithm to experimental data for a single α-helical trans-membrane domain of the channel-forming peptide

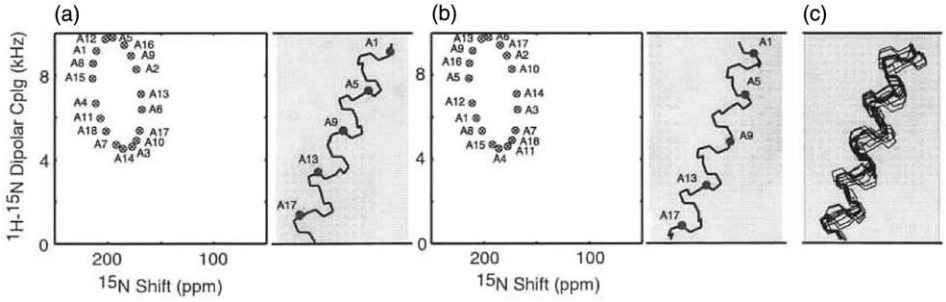

Fig. 3. Illustration of the fitting algorithm for the case of an ideal α-helix. (a) Choosing a relatively narrow range for the torsional angles, $\Phi = -65 \pm 5°$ and $\Psi = 40 \pm 5°$, yields unique structural fit (×) to the spectrum (○). (b) Increasing the fitting range to $\pm 10°$ yields another α-helical solution to the spectrum. (c) Superposition of 10 other possible α-helical solutions.

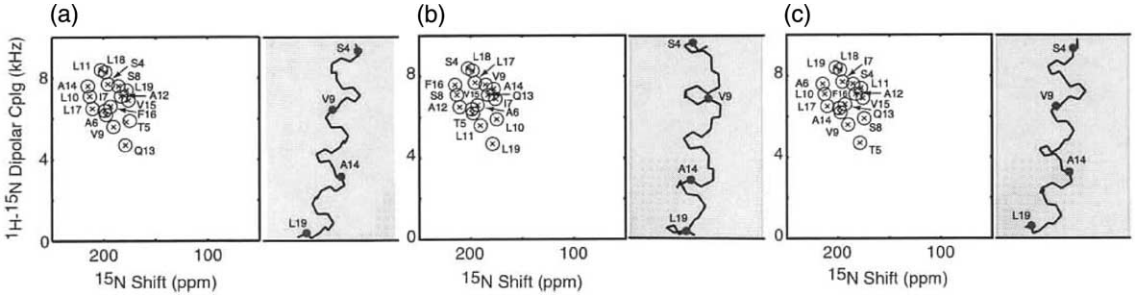

Fig. 4. Application to an experimental spectrum of AchR M2 (16 residues). (a) Completely assigned spectrum from [13] with the corresponding structural fit. (b) Assignment-free calculation #1. (c) Assignment-free calculation #2. The spectral peaks are represented by circles (○) reflecting the uncertainty in the experimental data and the corresponding fit is given by (×). Comparison of the structural solutions of parts B and C with the "correct" structure of part A shows the necessity of including some assignment information to improve the consistency of the fits.

from the acetylcholine receptor (S4-TAISVLLAQAV FLL-L19) [12]. First, the structure was calculated according to the original experimental assignment of the PISEMA spectrum shown in Fig. 4a. Then the spectrum was fit in an "assignment-free" manner. The results from two random shuffles of the spectral ordering are shown in Figs. 4b and c with the corresponding assignments and structures. During the fitting, the torsional angle Φ was allowed to vary between $-30°$ and $-80°$, whereas Ψ was varied from $-15°$ to $-75°$. Such a broad input range for the torsional angles is used with experimental data to ensure any kinks or bends in the structure are not missed. However, the solution is first sought near $\Phi = -65°$, $\Psi = -40°$ for each residue and the majority of the solutions indeed turn out to be close (to within 10–15°) to the ideal α-helical conformation. The size of the circles in Fig. 4 reflects the estimated experimental error (±300 Hz) in the NMR data. The structure in Fig. 4b is somewhat different from the "correct" structure of part Fig. 4a, although the structure in Fig. 4c is quite similar to that in Fig. 4a. However, the resonance assignments of the spectra in Figs. 4B and C are very different from the experimental resonance assignments in part A. The difference between the structural fits of parts B and C may be due not only to the allowed variations in Φ and Ψ, but also to the experimental error. To improve the convergence of the fits, some assignment information was incorporated into the structural fitting algorithm.

The resonances from the Ala, Val, and Leu residues were designated by residue type in accordance with the experimental assignments [13]; whereas the remaining residues are fit as described above. No information about sequential assignments was used; for example, the resonances for A6, A12, and A14 were only designated as arising from an alanine regardless of the residue number. Fig. 5a shows the resulting structural fit with the corresponding structure on the right. The assignments vary somewhat, but the structure in Fig. 5a is very similar to that in Fig. 4a based on complete sequential assignments. As was previously done for the data in Fig. 3c, 10 random shuffles of the order of the resonances were used to generate more possible assignments of the spectrum in Fig. 5a. The structural fits shown in Fig. 5b have RMSDs of 1.6 Å or less. Ala 14 is shown below Fig. 5b to give an impression of the accuracy of the determination of the helix twist. If no assignment information is used,

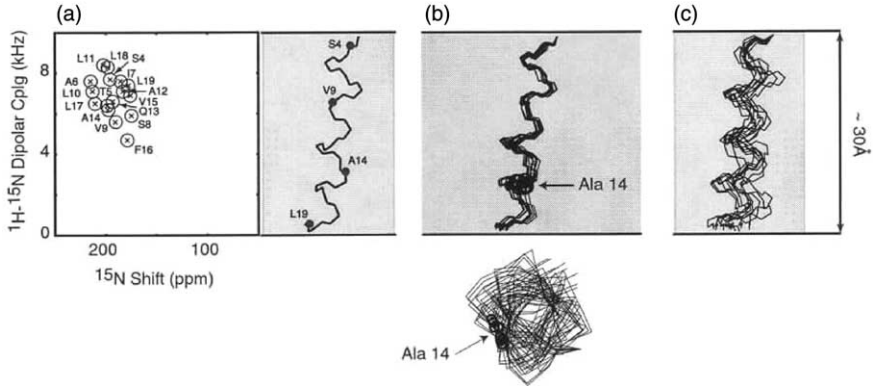

Fig. 5. Fitting of M2 data with restricted choices for Ala, Val, and Leu. (a) A possible spectral assignment of the data (○) with the corresponding fit (×). (b) Using selective labeling increases the consistency of the possible structures with RMSDs from 0.7 to 1.6 Å. Ala 14 is shown for each of the possible structures to illustrate the helix twist. (c) No assignment information results in greater RMSDs ranging from 1.8 to 2.2 Å.

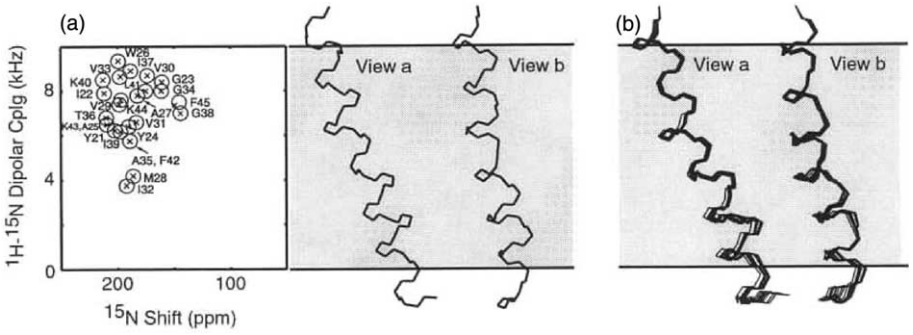

Fig. 6. Application to experimental data of fd-coat protein (25 residues). (a) Completely assigned spectrum from [14] with the corresponding structure. (b) Assignment-free structural fits with restricted choices for Ala, Val, Leu, Ile, Phe, and Gly. Helical solutions to the spectrum are viewed in both parts from two different angles *a* and *b* to show that the overall helical structure is retained even if only partial assignments are used.

RMSDs for the possible structural solutions are expected to be much greater. This is illustrated in Fig. 5c showing 10 possible fits resulting from 10 random shuffles of the peak ordering. Their RMSDs range from 1.8 to 2.2 Å.

Fig. 6 shows the fit to another helical domain, the trans-membrane helix of the fd-coat protein (Y21-IGYAWAMVVVIVGATIGIKLFKK-F45). Similar to Fig. 4a, the structure was first calculated using the fully assigned spectrum [14], Fig. 6a. Using residue-type assignments obtained from selective labeling with Ala, Val, Leu, Ile, Phe, and Gly gave a consistent set of structures (Fig. 6b) with RMSDs between 0.65 and 1 Å. Here the torsional angle Φ was allowed to vary between $-40°$ and $-80°$, and Ψ was varied from $-20°$ to $-60°$. Two different views of the polypeptide, "a" and "b", show that even though the fitted assignments in Fig. 6b may vary from those of the experimentally assigned spectrum in Fig. 6a, partial assignment information yields a closed set of solutions that accurately describes the overall structure of the helix including its tilt, twist, and the presence of a distinct kink near residue 39 [14].

3. Conclusions

It is possible to fit a structure of a protein to its solid-state NMR spectrum. The algorithm finds resonance assignments as part of the fitting procedure. Unfavorable assignments are automatically eliminated, whereas plausible α-helical assignments result in a close set of structures. The torsional angles Φ and Ψ are the only degrees of freedom, simultaneously providing structural constraints that satisfy the corresponding region of the Ramachadran plot. This algorithm represents a structural refinement that can reveal, with a high accuracy, deviations from an ideal α-helix, also giving the orientation of the helix as a whole.

Acknowledgments

This research was supported by Grants PO1GM 56538, R37GM24266, and RO1GM29754 from the National Institute of General Medical Sciences and utilized the Resource for Solid-State NMR of Proteins supported by Grant P41RR09731 from the Biomedical Research Technology Program, National Center for Research Resources, National Institutes of Health.

References

[1] F.M. Marassi, S.J. Opella, A solid-state NMR index of helical membrane protein structure and topology, J. Magn. Reson. 144 (2000) 150–155.
[2] J. Wang, J. Denny, C. Tian, S. Kim, Y. Mo, F. Kovacs, Z. Song, K. Nishimura, Z. Gan, R. Fu, J.R. Quine, T.A. Cross, Imaging membrane protein helical wheels, J. Magn. Reson. 144 (2000) 162–167.
[3] C.H. Wu, A. Ramamoorthy, S.J. Opella, High-resolution heteronuclear dipolar solid-state NMR spectroscopy, J. Magn. Reson. A 109 (1994) 270–272.
[4] F.M. Marassi, A simple approach to membrane protein secondary structure and topology based on NMR spectroscopy, Biophys. J. 80 (2001) 994–1003.
[5] M. Bak, R. Schultz, T. Vosegaard, N.C. Nielsen, Specification and visualization of anisotropic interaction tensors in polypeptides and numerical simulations in biological solid-state NMR, J. Magn. Reson. 154 (2002) 28–45.
[6] S.J. Opella, P.L. Stewart, K.G. Valentine, Q. Rev. Biophys. 19 (1987) 7–49.
[7] J.K. Denny, J. Wang, T.A. Cross, J.R. Quine, PISEMA powder patterns and PISA wheels, J. Magn. Reson. 152 (2001) 217–226.
[8] G. Arfken, Mathematical Methods for Physicists, third ed., Academic Press, Orlando, 1985, 985pp.
[9] T.E. Creighton, Proteins: Structure and Molecular Properties, second ed., Freeman, New York, 1993, p. 507.
[10] C.H. Wu, A. Ramamoorthy, L.M. Gierash, S.J. Opella, Simultaneous characterization of the amide ^{1}H–^{15}N chemical shift interaction tensors in a peptide bond by three-dimensional solid-state NMR spectroscopy, J. Am. Chem. Soc. 117 (1995) 6148–6149.
[11] T.G. Oas, C.J. Hartzell, W. Dahlquist, G.P. Drobny, The amide ^{15}N chemical shift tensors of four peptides determined from c dipole-coupled chemical shift powder patterns, J. Am. Chem. Soc. 109 (1987) 5962–5966.

[12] P.L. Stewart, R. Tycko, S.J. Opella, Peptide backbone conformation by solid-state nuclear magnetic resonance spectroscopy, J. Chem. Soc. Faraday Trans. I 84 (1988) 3803–3819.
[13] S.J. Opella, F.M. Marassi, J.J. Gesell, A.P. Valente, Y. Kim, M. Oblatt-Montal, M. Montal, Structures of the M2 channel-lining segments from nicotinic acetylcholine and NMDA receptors by NMR spectroscopy, Nat. Struct. Biol. 6 (1999) 374–379.
[14] F.M. Marassi, S.J. Opella, Simultaneous assignment and structure determination of a membrane protein from NMR orientational restraints, Protein Science, in press.